

Reduced cortical inhibition in a mouse model of familial childhood absence epilepsy

Heneu O. Tan*, Christopher A. Reid*, Frank N. Single†, Philip J. Davies*, Cindy Chiu*, Susan Murphy*, Alison L. Clarke*, Leanne Dibbens‡, Heinz Krestel§, John C. Mulley¶, Mathew V. Jones||, Peter H. Seeburg†, Bert Sakmann**††, Samuel F. Berkovic**‡, Rolf Sprengel†, and Steven Petrou*††

*Howard Florey Institute, University of Melbourne, Parkville 3010, Australia; †Department of Molecular Neurobiology and **Department of Cell Physiology, Max Planck Institute for Medical Research, 69120 Heidelberg, Germany; ‡Department of Genetic Medicine, Women's and Children's Hospital, Adelaide SA 5006, Australia; §Bionomics Limited, Thebarton, SA 5031, Australia; ¶Institute for Pharmacology and Toxicology, University of Zurich, Winterthurerstrasse 190, CH-8057 Zurich, Switzerland; ||Department of Physiology, University of Wisconsin, Madison, WI 53706; and ††Epilepsy Research Centre and Department of Medicine (Neurology), University of Melbourne and Austin Health, Melbourne, Heidelberg West VIC 3081, Australia

Contributed by Bert Sakmann, September 7, 2007 (sent for review February 18, 2007)

Mutations in the GABA_A receptor $\gamma 2$ subunit are associated with childhood absence epilepsy and febrile seizures. To understand better the molecular basis of absence epilepsy in man, we developed a mouse model harboring a $\gamma 2$ subunit point mutation (R43Q) found in a large Australian family. Mice heterozygous for the mutation demonstrated behavioral arrest associated with 6- to 7-Hz spike-and-wave discharges, which are blocked by ethosuximide, a first-line treatment for absence epilepsy in man. Seizures in the mouse showed an abrupt onset at around age 20 days corresponding to the childhood nature of this disease. Reduced cell surface expression of $\gamma 2$ (R43Q) was seen in heterozygous mice in the absence of any change in $\alpha 1$ subunit surface expression, ruling out a dominant-negative effect. GABA_A-mediated synaptic currents recorded from cortical pyramidal neurons revealed a small but significant reduction that was not seen in the reticular or ventrobasal thalamic nuclei. We hypothesize that a subtle reduction in cortical inhibition underlies childhood absence epilepsy seen in humans harboring the R43Q mutation.

GABA_A receptor | genetics | electroencephalogram | trafficking | synapse

GABA_A receptors in the adult brain are important for inhibiting the activity of neurons in which they reside. Dysfunction of these receptors caused by familial mutations can give rise to febrile seizures (FS) and a variety of generalized epilepsy phenotypes (1–3). To date, five mutations have been reported in the GABA_A $\gamma 2$ subunit gene with an array of seizure types seen in patients (1, 4–7). Childhood absence epilepsy (CAE) and FS were the main phenotypes in a large Australian family with an arginine to glutamine mutation at position 43 (R43Q) in the GABA_A $\gamma 2$ subunit gene (1, 8).

Understanding how the GABA_A $\gamma 2$ (R43Q) mutation causes epilepsy is difficult. GABA_A receptors themselves serve several roles. They regulate moment-to-moment brain function (9), play an important role in brain development (10), and have key roles in neuronal plasticity (11, 12) and response to brain injury (13–15). Epilepsy itself is a complex phenomenon involving the interaction of multiple cell types in networks within and between different brain regions that are likely to be influenced by GABA_A receptor dysfunction caused by the R43Q mutation. Furthermore, *in vitro* analyses of the consequences of this mutation have shown inconsistent findings with a range of deficits in receptor pharmacology, trafficking, kinetics, or assembly (16–23) potentially implicated in disease pathogenesis.

Clearly, the complex nature of epileptogenesis demands *in vivo* investigation. Genetic epilepsies provide a framework on which to investigate the consequences of causative mutations at a range of organizational levels within the brain, creating a chain of understanding from molecules to behavior. Linking this chain is impossible in humans because of the highly invasive methodology required and is severely limited in heterologous expression systems that lack necessary complexity. Mice models harboring homologous human pathogenic mutations and displaying shared phenotypic

features with patients provide a unique opportunity to investigate molecular, synaptic, network, and behavioral aspects of clinically relevant epileptogenesis.

Here, we report on the creation and analysis of a mouse model with the homologous GABA_A $\gamma 2$ (R43Q) point mutation found in an Australian family with FS and CAE (1, 8). These mice recapitulate the primary seizure phenotype observed in patients, and electrophysiological characterization suggests that the mutation results in a subtle reduction of synaptic cortical inhibition, supporting the idea that absence seizures are initiated through hyperexcitability within the cortex (24).

Results

Construction of Mouse Model. GABA_A $\gamma 2$ (R43Q) mutant mice were constructed by homologous recombination in R1 ES cells of a targeting vector made with SV 129-derived genomic DNA. The R43Q mutation was introduced together with four silent mutations (Fig. 1*a*). Targeted clones were identified by using PCR screening and confirmed with Southern blotting (Fig. 1*b*). Blastocysts were injected with ES cells and implanted. Chimeric mice were bred with a “Cre deleter” strain (25) and screened for germ line transmission. For genetic background studies, a minimum of eight backcrosses were performed. Mice were routinely genotyped by using PCR of tail DNA (Fig. 1*c*).

Cre excision results in the intronic retention of a single LoxP site that may interfere with transcription. Quantitative real-time PCR was used on total brain RNA from heterozygous mice ($n = 4$) to assess the potential effects of this LoxP site on transcript levels. mRNA levels of the Gln-43 allele containing the LoxP site and wild-type Arg-43 allele were identical (Fig. 1*d*).

Western blot analyses of total $\gamma 2$ were performed on wild-type ($n = 10$), heterozygous ($n = 15$), and homozygous ($n = 9$) forebrains at embryonic day (E) 16 (Fig. 1*e*). There was a significant ($P = 0.025$) reduction in total $\gamma 2$ levels in homozygous mice, with no change seen in heterozygotes. This finding suggests that the $\gamma 2$ (Q43) protein is made, albeit less $\gamma 2$ (R43) and that the $\gamma 2$ (R43)

Author contributions: H.O.T., C.A.R., and S.P. designed research; H.O.T., C.A.R., F.N.S., P.J.D., C.C., S.M., A.L.C., and S.P. performed research; L.D., H.K., J.C.M., M.V.J., P.H.S., B.S., and R.S. contributed new reagents/analytic tools; H.O.T., C.A.R., P.J.D., C.C., and S.P. analyzed data; and H.O.T., C.A.R., S.F.B., and S.P. wrote the paper.

Conflict of interest statement: S.P., S.F.B., and J.C.M. were paid consultants of Bionomics Limited, which holds the intellectual property around this project.

Abbreviations: CAE, childhood absence epilepsy; E, embryonic day; EEG, electroencephalogram; FS, febrile seizures; IPSC, inhibitory postsynaptic current; m, miniature; P, postnatal day; PTZ, pentylenetetrazol; scPTZ, subcutaneous PTZ; s, spontaneous; SWD, spike-and-wave discharge; TRN, thalamic reticular nucleus; VB, ventrobasal thalamus.

††To whom correspondence may be addressed. E-mail: sakmann@mpimf-heidelberg.mpg.de or spetrou@unimelb.edu.au.

This article contains supporting information online at www.pnas.org/cgi/content/full/0708440104/DC1.

© 2007 by The National Academy of Sciences of the USA

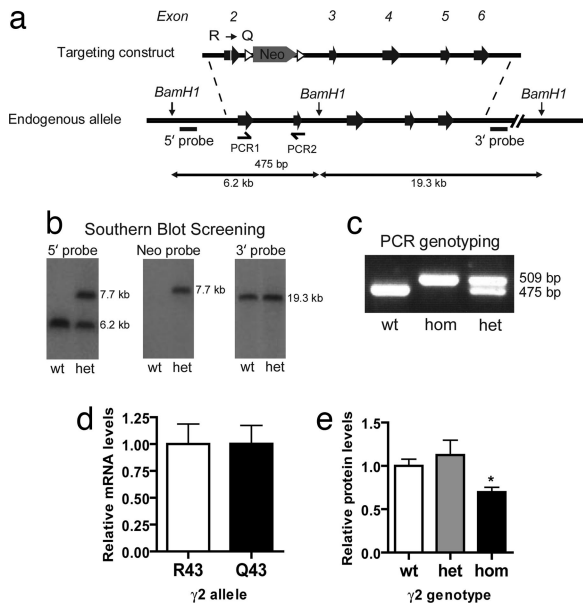


Fig. 1. Generation of the GABA_A γ 2(R43Q) mutant mouse. (a) Schematic of the targeting construct. (b) Southern blot analysis of genomic DNA from ES cell colonies indicating the desired recombination event. (c) PCR genotyping analysis of genomic DNA from the offspring of a heterozygous intercross. (d) Quantitative real-time PCR of mutant and wild-type alleles. (e) Western blot analysis of γ 2 subunits in brain homogenates from wild-type (wt), heterozygous (het), and homozygous (hom) P14 mice. *, $P < 0.05$.

allele must, therefore, be up-regulated to bring total γ 2 in the heterozygous mice to wild-type levels (Fig. 1e).

Heterozygous mice from both strains thrived and did not show any neurological overt signs or convulsive seizures. However, homozygous mice were rarely born, and when they were, they possessed altered gaits, a severe tremor, and died before postnatal day (P) 19.

GABA_A γ 2(R43Q) Mice Display an Absence Epilepsy Phenotype That Can Be Modified by Genetic Background. CAE and FS are the major clinical phenotypes of patients heterozygous for the γ 2(R43Q) mutation (8, 26). Clinically, CAE is characterized by sudden behavioral arrest associated with 3- to 4-Hz spike-and-wave discharges (SWDs) on EEG (26). We specifically assessed for spontaneous absence epilepsy by using video-EEG analysis in awake and freely moving mice. Behavioral arrest with SWD on EEG was confirmed in >50 heterozygous mice (Fig. 2). For a typical video-EEG phenotype, see [supporting information \(SI\) Movie 1](#).

SWDs had a typical burst frequency ranging between 5 and 8 Hz and high-amplitude (500–1,100 μ V) with limited spike-to-spike variability. SWDs occurred in heterozygous mice in all vigilance states, up to 50 times per h and were variable. The behavioral component of seizures was most striking when they occurred during periods of intense activity, during which the mice would display an obvious pause for the duration of the SWD. On occasion, behavioral arrest extended beyond the period of the SWD. Some mice also displayed stereotypical nodding and twitching of the orofacial region during SWDs with yet others showing a seizure offset accompanied by a subtle jerk or turn of the head. We did not detect absence-like seizures in wild-type mice ($n = 16$; Fig. 2), nor did we see the pathological SWDs. EEGs from homozygous mice ($n = 2$) lacked normal brain rhythms indicative of severe neurological dysfunction (Fig. 2a).

Clinical heterogeneity of γ 2(R43Q) patients was evident with incomplete penetrance and phenotypic variability, suggesting modulation genetic factors (1, 8). To determine the effects of genetic

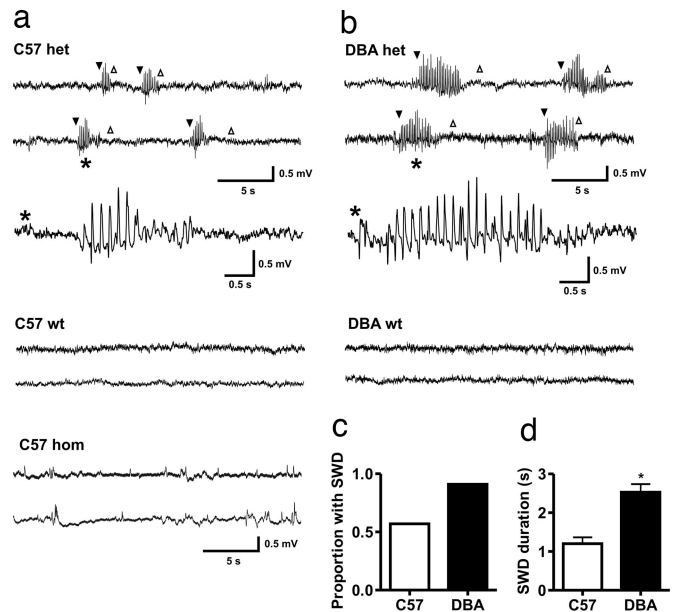


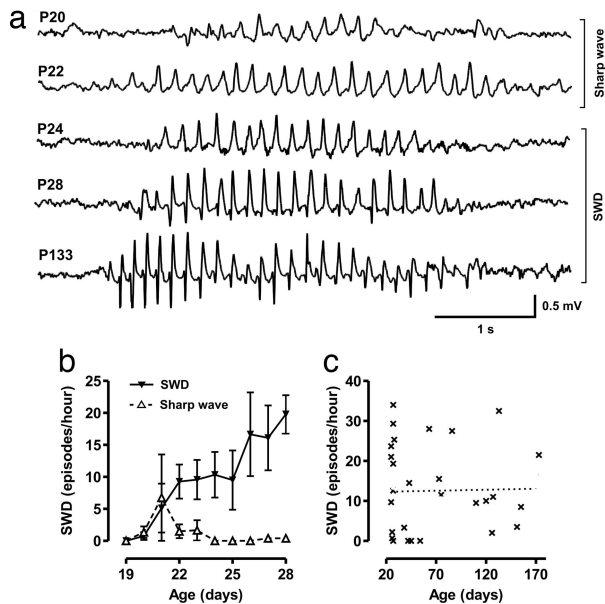
Fig. 2. Spontaneous absence seizures recorded electrographically and behaviorally in two genetic strains harboring the R43Q mutation. EEGs recorded from wild-type (wt), heterozygous (het), and homozygous (hom) mutants in the C57BL/6 (a) or DBA/2J (b) genetic background. Onset of behavioral arrest is indicated by filled triangles, and cessation is indicated by open triangles. Asterisk indicates expanded trace. (c) Proportion of heterozygote C57BL/6 and DBA/2J mice that showed SWD with behavioral arrest. (d) Average duration of a SWD episode in C57BL/6 and DBA/2J mice. *, $P = 0.002$.

modifiers on the mouse, we bred into both C57BL/6 and DBA/2J genetic backgrounds. These strains have the highest and least resistance to seizures, respectively, among commonly used mice lines (27). DBA/2J strains were also chosen because they exhibit nonepileptic brief spindle episodes that do not occur in C57BL/6 (28). An obvious strain difference was noted between heterozygous mice from the C57BL/6 and DBA/2J backgrounds (Fig. 2a and b). Penetrance of the GABA_A γ 2(R43Q) mutation was greater in the DBA/2J strain compared with C57BL/6 with >90% of P25–P28 mice tested showing symptomatic SWDs (Fig. 2c). Furthermore, the duration of each SWD episode was significantly longer in the DBA/2J (2.53 ± 0.21 ms; $n = 10$ mice from 48 SWD; $P < 0.01$) compared with C57BL/6 mice (1.20 ± 0.16 ms; $n = 4$ mice from 44 SWD; Fig. 2d). SWDs from the two different strains were similar in all other respects, including spiking frequency, amplitude, and rate of occurrence of SWD episodes (SI Table 1).

Development of Absence Epilepsy in the GABA_A γ 2(R43Q) Mouse.

CAE has a very characteristic age dependence, with onset occurring between 3 and 8 years of age (26). To determine the age dependence of seizures in the mouse model, EEGs from DBA/2J mice were recorded (Fig. 3). Abnormal paroxysmal discharges, first noted at P20, were characterized by irregular low-amplitude sharp waves that were not associated with any discernable change in vigilance. By P22, the amplitudes of the sharp waves had increased, were more regular, and, on some occasions, were associated with behavioral arrest. Frank epileptiform discharges occurred by P24–P28 with a distinct spikes and wave morphology associated with behavioral arrest (Fig. 3a and b).

Remission of absence epilepsy at puberty is a common clinical observation, although persistence into adulthood may occur (29). To assess the possible age dependence of seizure remission in the GABA_A γ 2(R43Q) mouse, we performed video-EEG analysis across a range of ages. SWDs and behavioral arrest were observed with no obvious change in incidence across time (Fig. 3c).



Absence Seizures Are Reduced by Ethosuximide. Ethosuximide is a first-line treatment for CAE and is also one of the benchmarks for validating rodent models of absence epilepsy. Ethosuximide (200 mg·kg⁻¹ i.p.) (30) reduced SWDs in heterozygous DBA/2J mice (Fig. 4).

Reduced Proconvulsant Seizure Threshold. Pentylentetrazol (PTZ) is a proconvulsant that blocks GABA_A receptors and provides a global measure of network excitability and seizure susceptibility. C57BL/6 mice were s.c. injected with PTZ (scPTZ; 85 mg·kg⁻¹) and monitored for the time to the first clonic seizure (Fig. 5a) and tonic hindlimb extension (Fig. 5b). The GABA_A γ 2(R43Q) mice ($n = 22$) were significantly more sensitive to scPTZ and reached both end points more rapidly than did wild type ($n = 16$).

Synaptic Inhibition Is Specifically Reduced in Layer 2/3 Pyramidal Neurons of the GABA_A γ 2(R43Q) Mouse. Pathological oscillations of the thalamocortical circuit are a hallmark of absence seizures (31). This circuit comprises the somatosensory cortex, thalamic reticular nucleus (TRN) and ventrobasal thalamus (VB) (32). GABAergic inhibition plays important and distinct roles in each of these nuclei,

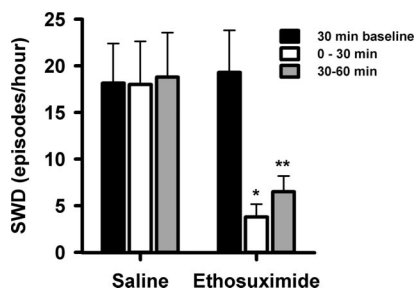


Fig. 4. Ethosuximide (200 mg·kg⁻¹) reduces the average number of SWDs in the GABA_A γ 2(R43Q) mouse ($n = 14$). *, $P < 0.001$; **, $P < 0.01$.

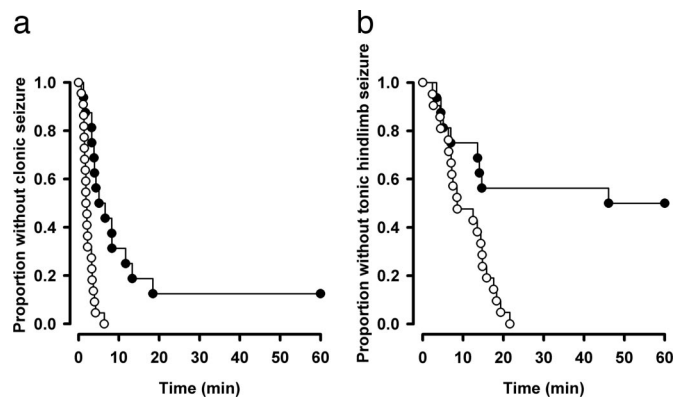


Fig. 5. Heightened susceptibility to scPTZ. Survival curves for wild-type and heterozygous GABA_A γ 2(R43Q) mice in the C57BL/6 background after s.c. administration of PTZ (85 mg·kg⁻¹). After scPTZ administration, heterozygous mice (open circles) progressed more rapidly to clonic seizures (a) and tonic hindlimb seizures (b) than did wild type (filled circles) (clonic, $P < 0.001$; tonic hindlimb extension, $P = 0.001$; Logrank test).

implicating these regions in the pathogenesis of absence epilepsy in the GABA_A γ 2(R43Q) model. Analysis of miniature (m) or spontaneous (s) inhibitory postsynaptic currents (IPSCs) were made in brain slices from P14–P16 mice. Within this developmental window, GABA_A receptor subunit expression profiles have stabilized (33), and importantly, SWDs and behavioral seizures are not evident, eliminating the confound of plasticity/kindling caused by seizure activity. GABA_A receptor-mediated mIPSCs were recorded from layer 2/3 pyramidal neurons (Fig. 6a) and revealed a potentially important change in synaptic inhibition. mIPSC amplitude was significantly lower in the GABA_A γ 2(R43Q) mice com-

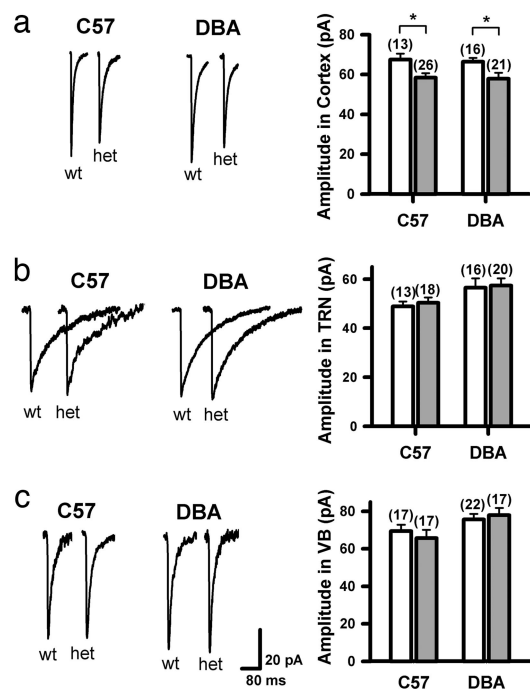


Fig. 6. A deficit in cortical inhibition is common to C57/BL6 and DBA/2J mutant mice. (a) Averaged mIPSCs from single layer 2/3 pyramidal neurons with pooled averages. (b) mIPSCs from single TRN neurons with pooled averages. Note that the slower decay kinetics of these synaptic events is typical of inhibitory currents in the TRN. (c) Averaged sIPSCs from single VB neurons with pooled averages. *, $P < 0.05$.

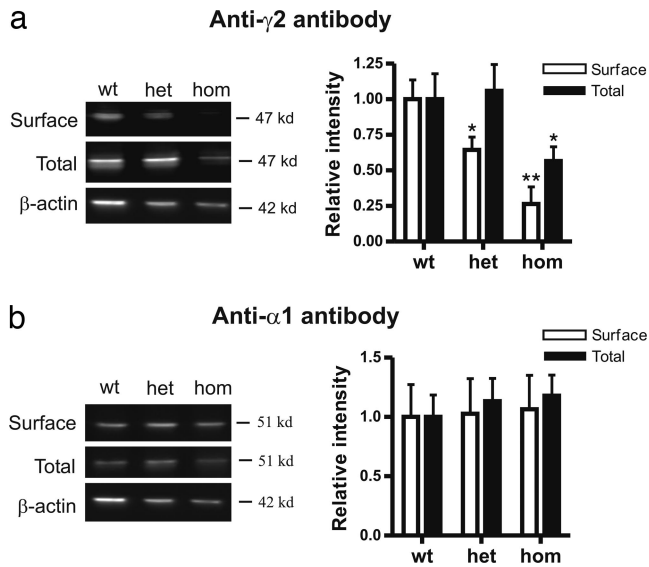


Fig. 7. Specific reduction in cell surface expression of $\gamma 2$ (R43Q) subunits. Western blot analysis of cell surface and total protein levels in neurons cultured from wild-type (wt), heterozygous (het), and homozygous (hom) embryos is shown. (a) Immunoblots using antibodies specific to $\gamma 2$ and β -actin. Normalized surface (open bars) and total (filled bars) $\gamma 2$ expression is shown. (b) Immunoblots using GABA_A $\alpha 1$ antibodies. Normalized surface (open bars) and total (filled bars) $\gamma 2$ expression is shown. *, $P < 0.05$; **, $P < 0.01$.

pared with wild-type in both the C57BL/6 (wild type, 67.5 ± 2.9 pA; heterozygous, 58.4 ± 2.2 pA; $P = 0.03$) and DBA/2J (wild type, 66.4 ± 1.8 pA; heterozygous, 57.9 ± 2.9 pA; $P = 0.01$) genetic backgrounds. Because mIPSCs frequency was low in the TRN and VB, sIPSCs were recorded. Regions were identified by anatomical position within the brain slice (34), distinctive dendritic morphology as shown by intracellular staining with biocytin (data not shown), and distinctive current kinetics (Fig. 6). In contrast to the changes seen in the cortical neurons, there were no significant differences in amplitudes of sIPSCs in the TRN (Fig. 6b) or the VB (Fig. 6c) in either genetic strain. These data show a specific deficit in inhibitory efficacy in the somatosensory cortex that may be responsible for the generation of absence seizures.

$\gamma 2$ (R43Q) Subunits Have Reduced Cell Surface Expression and Do Not Associate with $\alpha 1$ Subunits in Cultured Cortical Neurons. The reduced cortical mIPSCs described above could be explained by intracellular retention of receptors comprising the mutant $\gamma 2$ (R43Q) subunit. This possibility has been raised in studies that used cell culture systems to heterologously express mutant subunits and assess function and membrane trafficking (16, 19, 20). To determine whether incorporation of the $\gamma 2$ (R43Q) subunit causes retention of GABA_A receptor complexes by a dominant-negative effect, we cultured primary neurons from C57BL/6 embryonic cortices (E15–E16) and biotin-labeled cell surface receptors. Immunoblots with an antibody against $\gamma 2$ (Fig. 7a) and $\alpha 1$ (Fig. 7b) subunits were made on surface as well as total protein fractions obtained after 15 days in culture. Analysis of cultured neurons from heterozygous GABA_A $\gamma 2$ (R43Q) mice showed a significant reduction in $\gamma 2$ subunit cell surface expression (normalized density, 0.64 ± 0.09 ; $n = 6$) compared with wild type (normalized density, 1.00 ± 0.12 ; $n = 6$; $P = 0.026$). This deficit was even greater in cultures from homozygous mice (normalized density, 0.26 ± 0.12 ; $n = 5$; $P < 0.017$). Total protein expression provides a measure of protein synthesis and degradation. Interestingly, we only detected a change in total $\gamma 2$ subunit levels in homozygous cultures (normalized density, 0.57 ± 0.10 ; $n = 6$; $P = 0.035$), which suggests that degradation processes inside the neurons preferentially remove

mutant $\gamma 2$ subunits. A dominant-negative mutation that causes retention would be expected to also reduce cell surface expression of α subunits. There was no detectable change in $\alpha 1$ subunit expression in heterozygous or homozygous cultures, suggesting that a simple dominant-negative mechanism is unlikely to explain the observed seizure phenotype.

Discussion

Heterozygous Mice Recapitulate the Human Phenotype. CAE seen in the family with the R43Q mutation is typical (8), supporting the concept that rare mutations can give rise to common forms of epilepsy. The GABA_A $\gamma 2$ (R43Q) mouse recapitulates the clinical phenotype in five ways. First, it spontaneously exhibits rhythmic SWDs on its EEG associated with behavioral arrest, the clinical hallmarks of CAE. Second, seizures are responsive to a first-line antiabsence epilepsy drug, ethosuximide. Third, onset of absence seizures occurs at a young age similar to CAE. Fourth, we detected a decrease in cortical benzodiazepine receptor density, analogous to the reduction in binding potential of PET-labeled flumazenil in the cortex of R43Q patients (21). Finally, the seizure phenotype of the GABA_A $\gamma 2$ (R43Q) mouse is influenced by genetic background, which may reflect the clinical heterogeneity seen in the R43Q family pedigree (1). This finding is in agreement with the complex monogenic mode of inheritance proposed by Wallace and colleagues (1) and other investigators (2) in which the mutation is necessary but not sufficient to manifest epilepsy.

The few homozygous GABA_A $\gamma 2$ (R43Q) mice that were born died before P18, supporting the idea that a normally functioning $\gamma 2$ subunit is vital (35). Furthermore, the observed lethality of the homozygous state demonstrates unequivocally that the mutation changes the molecular properties of GABA receptors.

Development of SWDs: Witnessing Epileptogenesis? One of the characteristic features of CAE is its distinctive onset, in childhood at ≈ 3 –8 years of age (26). The GABA_A $\gamma 2$ (R43Q) mouse also shows a stereotypic early and rapid onset (P19–P21). In the mouse, the paroxysmal discharge morphology develops from rhythmic high-amplitude bursts of sharply contoured waves to frank epileptiform SWD, which may be a marker of the underlying pathological process that gives rise to absence seizures. The first 2 weeks in the life of a mouse roughly correspond to the early childhood development years (36). In both mouse and human, this period represents a time when intense neurodevelopmental changes are under way. The timing of onset may provide clues as to what coincident developmental processes are relevant to the mechanism of epileptogenesis in this model. Layering and somatotopic map formation in the somatosensory cortex are completed by the 1st postnatal week (37). Furthermore, development of the thalamocortical circuit and GABAergic inhibition is thought to be predominantly completed during embryonic stages (E13–E18). This theory raises the possibility that the R43Q mutation could alter morphology and connectivity of thalamocortical neurons, although in this context the trigger for seizures would likely be the response of this altered network to a normal developmental event. The expression profile of GABA_A receptor subunits is dynamic around this time, stabilizing around the 2nd postnatal week (33). Also, the developmental shift from depolarizing to hyperpolarizing GABA_A responses, caused by a KCC2-triggered shift in Cl⁻ reversal, occurs in this early postnatal stage of life (38). Although these developmental processes do not have a time course that exactly parallel the onset of SWDs, they are candidates worthy of investigation in the mouse model.

$\gamma 2$ (R43Q) Cell Surface Reduction Is Common to Mouse and Man. Evidence for reduced benzodiazepine receptor cell surface expression has been reported in the R43Q family, where flumazenil-binding potential was reduced compared with family members without the mutation (21). Our results suggest that reduced binding

potential to flumazenil, a benzodiazepine receptor antagonist, is caused, at least in part, by a reduction in $\gamma 2$ (R43Q) subunit surface expression.

The cortical deficit in synaptic inhibition is readily attributable to the consequences of reduced cell surface expression of the $\gamma 2$ (R43Q) subunit with no effect on $\alpha 1$ subunit cell surface expression. The implication from these findings is that $\gamma 2$ (R43Q) is not efficiently assembling into mature receptors and is thus not dominant-negative but simply reduced in abundance. A loss of $\gamma 2$ (R43Q) may cause a deficit in synaptic inhibition by allowing other subunits to incorporate into GABA_A receptors. These new receptors may have altered kinetics or pharmacology that could impinge on function even beyond the measures made in the present work. Furthermore, loss of $\gamma 2$ (R43Q) could alter trafficking (39) such that density of receptors at synapses is reduced, causing the observed reduction in mIPSCs. In partial contrast to our *in vivo* finding, heterologous expression studies performed in HEK cells demonstrate both a reduction in $\gamma 2$ subunit expression and in fully formed heteromeric GABA_A receptors at the cell surface, suggesting a dominant-negative effect of the R43Q mutation (16, 18–20). These studies highlight a need for caution when using the results from cell-based experiments to explain the genesis of complex diseases.

Is Reduced Cortical Inhibition Sufficient to Cause Absence Epilepsy?

Reduced synaptic inhibition was localized to the somatosensory cortex (pyramidal neurons in layers 2/3) with no change seen in the TRN and VB. Importantly, genetic background had no influence on this pattern, suggesting a strong penetrance of this synaptic phenotype associated with the R43Q mutation. Our findings, in a clinically based genetic model of absence epilepsy, support the cortical hypothesis for the site of the primary defect. A very influential hypothesis of a deep midline centrencephalic origin was posited for SWDs in the 1940s, but evidence gradually built up from a number of sources that the cerebral cortex was the primary generator, albeit influenced by thalamocortical volleys (40, 41). Indeed, recent evidence from a rat model implicates the perial region of the somatosensory cortex in initiating SWDs (24). Interestingly, R43Q family members also had a specific reduction in cortical flumazenil-binding potential, further highlighting the potential importance of this region in the epileptogenic process. Moreover, reduced GABAergic cortical inhibition has been inferred from human studies using paired-pulse transcranial magnetic stimulation in idiopathic generalized epilepsy (42) and specifically in patients with the R43Q mutation (55).

Layer 2/3 neurons recorded in our work form local cortical microcircuits and do not make direct projections to the thalamus. However, there is anatomical and functional evidence for connectivity between layer 2/3 pyramidal neurons and the deeper layer 5 pyramidal neurons, which themselves project to layer 6 corticothalamic neurons (43, 44). Because thalamic bursting, which drives sleep spindles and the pathology of SWDs, is sensitive to cortical input (45), it is possible that changes in the properties of local microcircuits in layer 2/3 could drive changes in input to the thalamus and thereby trigger the pathological 6 Hz SWDs seen in our model. Although not examined in this work, dysfunction in GABAergic synapses of other layers within the cortex or changes in non-GABA_A-mediated properties may also contribute to development of seizures in this model.

Genetic Syndrome-Specific Mouse Models of Epilepsy: Are They Clinically Relevant? There are several genetic models of absence epilepsy in rodents. The most commonly used of these models are the genetic absence epilepsy rat from Strasbourg (GAERS) rat (46), Wistar albino Glaxo from Rijswijk (WAG/Rij) rats (47), and more recently, C3H/He mice (30). While these models exhibit absence seizures, their polygenic mode of inheritance makes it difficult to find the genetic mechanisms responsible for the disease. Although

several physiological abnormalities in these models have been associated with their pathology (48–51), it is difficult to confirm whether these findings reflect causal or adaptive processes in the brain or even perhaps epiphenomena. There are also several monogenic mice models of absence epilepsy such as tottering, lethargic, and stargazer, which have known Ca²⁺ channel mutations (26). Phenotypically, however, there are departures from typical absence epilepsy with the presence of either ataxia or other movement disorders that are not observed in absence epilepsy. Syndrome-specific epilepsy models based on known human genetic lesions, which recapitulate human phenotypes, may provide a more powerful means to understanding the underlying basis of human epilepsy.

Methods

Construction of the Mouse Model. The gene replacement targeting vector was assembled with a neomycin-positive selection marker and flanking 129/Sv genomic DNA (Fig. 1a). The R43Q mutation, plus four other silent mutations (data not shown), were introduced into exon 2 by using overlapping PCR primers. The final targeting vector comprised ≈ 1.1 kb of 5' and ≈ 8 kb of 3' sequences. Linearized vector was electroporated into R1ES cells (52) as described previously (53) selected with G418 (250 μ g/ml). Colonies were screened by PCR and Southern blotting (Fig. 1b) to confirm targeting.

ES cells were injected into C57BL/6 blastocysts, and chimeras were backcrossed to C57BL/6 mice. Cre excision of the neomycin cassette was achieved by crossing $\gamma 2^{R43/Q43neo}$ mice with a Cre-transgenic deleter strain (25).

Real-Time RT-PCR. Total RNA was extracted from heterozygous mice (P15) brains ($n = 4$) and reverse-transcribed into cDNA. TaqMan probes complementary to the genomic region containing the mutation were designed so that wild-type probe and mutant probes differed only by the R43Q mutation and four silent mutations introduced into the adjacent sequence. Nonmultiplex real-time PCR was performed in an ABI PRISM 7700 (Applied Biosystems, Foster City, CA). For endogenous control, PCR was also performed on the same plate by using 1 \times Platinum SYBR Green qPCR Supermix (Invitrogen, Carlsbad, CA) with forward and reverse primers for 18S rRNA.

EEG Recordings. Mice were anesthetized with 1–3% isoflurane and implanted with epidural EEG electrodes. Signals were low-pass filtered at 200 Hz, AC-coupled at 0.1 Hz, and sampled at 1 kHz with Powerlab 16/30 (ADInstruments, Colorado Springs, CO) with synchronized video monitoring.

scPTZ. Mice between 24 and 28 days old were injected with PTZ (85 mg \cdot kg⁻¹) and video-monitored for 1 h. Latencies to minimal (clonic) and maximal (tonic hindlimb extension) seizures were recorded.

Electrophysiological Recording. Cortical brain slices (300 μ m thick) were cut in the parasagittal plane. Thalamocortical slices (300 μ m thick) obtained as described by Agmon and Connors (34) were used for recordings from TRN and VB. Recordings were made at 34°C, and slices were perfused with artificial CSF solution consisting of 125 mM NaCl/2.5 mM KCl/25 mM NaHCO₃/1.25 mM NaH₂PO₄/1 mM MgCl₂/2 mM CaCl₂/10 mM glucose, aerated with 95% O₂/5% CO₂ to a final pH of 7.4. Ten micromolar 6-cyano-7-nitroquinoxaline-2,3-dione sodium (CNQX) and 30 μ M D(-)-2-amino-5-phosphonovaleric acid (APV) were used to block glutamatergic currents, and 0.5 μ M tetrodotoxin was used to block sodium currents. Residual currents were bicuculline-sensitive ($n = 3$, 40 μ M). Electrodes contained 105 mM CsCl, 35 mM CsOH, 10 mM Hepes, 10 mM EGTA, mM 10 phosphocreatine, 4 mM ATP-Mg and 0.3 mM GTP-Na, 14 mM D-mannitol, 5 mM QX-315, and 8

mM biocytin hydrochloride at a final pH of 7.3 and osmolarity of 300 mOsm. All drugs were obtained from Sigma (St. Louis, MO).

Neurons were clamped at -70 mV after correction for liquid junction potential by using a MultiClamp 700A (Molecular Devices, Sunnyvale, CA). Spontaneous IPSCs were recorded in 60-s epochs and were low-pass filtered at 2 kHz and digitized at 10 KHz. Fifty to seventy percent series resistance compensation was used, and data were only included in analysis if the series resistance was <25 M Ω and did not change by $>20\%$ during the course of the recording.

Synaptic events were detected by using the template matching algorithm of pClamp 9.0 (Molecular Devices) and confirmed visually. Individual events were aligned on the rising phase to generate average representatives for each cell.

Biotinylation and Western Blot Analysis. Primary neurons from E15–E16 mice were cultured by using methods described previously (54). Neurons were plated at a density of 1×10^5 cells per cm^2 on poly-L-lysine-coated polystyrene culture flasks in neurobasal medium (Invitrogen) supplemented with 10% FCS, B-27 supplement (Invitrogen), and Glutamax (Invitrogen; 0.5 mM) in 95% O₂/5% CO₂ at 37°C. After 24 h, the medium was replaced with serum-free neurobasal medium supplemented with B-27 and left unchanged for 15 days.

Cell surface protein biotinylation and purification (Pierce Biotechnology, Rockford, IL) was used to obtain surface and total

fractions from embryonic cultures. Whole embryonic forebrains (E16) were also acutely dissociated and homogenized to obtain total forebrain lysate. Proteins were fractionated by using SDS/PAGE and immunoblotted with rabbit GABA_A receptor $\gamma 2$ (Alomone; 1:250) and $\alpha 1$ (Alomone; 1:250) antibodies. Mouse β -actin (Abcam; 1:30,000) was used to standardize protein loading between samples and to confirm specificity of biotinylation to cell surface proteins. ECL rabbit IgG from donkey (1:20,000; GE Healthcare, Piscataway, NJ) and ECL mouse IgG from sheep (1:50,000; GE Healthcare) conjugated with horseradish peroxidase was used as secondary antibody. Antibody reactivity was imaged by using ECL plus Western blotting reagent (GE Healthcare) and quantified by using a LAS-1000plus (Fujifilm, Brookvale, NSW, Australia).

Data Analysis. All group data are expressed as mean \pm SEM and compared by using either an unpaired Student's *t* test or Mann–Whitney nonparametric test unless otherwise indicated. $P < 0.05$ was taken as statistical significance (Prism; GraphPad Software, San Diego, CA).

We thank Khai See Tan for technical support and Dr. Evan Thomas for helpful discussions. This work was supported by Bionomics Limited, a National Health and Medical Research Council program grant (to S.P., S.F.B., and J.C.M.), and National Institutes of Health Grant NS046378 (to M.V.J. and S.P.).

- Wallace RH, Marini C, Petrou S, Harkin LA, Bowser DN, Panchal RG, Williams DA, Sutherland GR, Mulley JC, Scheffer IE, Berkovic SF (2001) *Nat Genet* 28:49–52.
- Steinlein OK (2002) *Eur J Pain* 6(Suppl A):27–34.
- Noebels JL (2003) *Annu Rev Neurosci* 26:599–625.
- Baulac S, Huberfeld G, Gourfinkel-An I, Mitropoulou G, Beranger A, Prud'homme JF, Baulac M, Brice A, Bruzzone R, LeGuern E (2001) *Nat Genet* 28:46–48.
- Harkin LA, Bowser DN, Dibbens LM, Singh R, Phillips F, Wallace RH, Richards MC, Williams DA, Mulley JC, Berkovic SF, et al. (2002) *Am J Hum Genet* 70:530–536.
- Kananura C, Haug K, Sander T, Runge U, Gu W, Hallmann K, Rebstock J, Heils A, Steinlein OK (2002) *Arch Neurol* 59:1137–1141.
- Audenaert D, Schwartz E, Claeys KG, Claes L, Deprez L, Suls A, Van Dyck T, Lagae L, Van Broeckhoven C, Macdonald RL, De Jonghe P (2006) *Neurology* 67:687–690.
- Marini C, Harkin LA, Wallace RH, Mulley JC, Scheffer IE, Berkovic SF (2003) *Brain* 126:230–240.
- Bormann J (2000) *Trends Pharmacol Sci* 21:16–19.
- Owens DF, Kriegstein AR (2002) *Nat Rev Neurosci* 3:715–727.
- Hensch TK (2005) *Nat Rev Neurosci* 6:877–888.
- Collingridge GL, Isaac JT, Wang YT (2004) *Nat Rev Neurosci* 5:952–962.
- Velasco I, Tapia R (2002) *J Neurosci Res* 67:406–410.
- Wang X, Shimizu-Sasamata M, Moskowitz MA, Newcomb R, Lo EH (2001) *Neurosci Lett* 313:121–124.
- Stellwagen D, Beattie EC, Seo JY, Malenka RC (2005) *J Neurosci* 25:3219–3228.
- Sancar F, Czajkowski C (2004) *J Biol Chem* 279:47034–47039.
- Macdonald RL, Bianchi MT, Feng H (2003) *Exp Neurol* 184(Suppl 1):S58–S67.
- Kang JQ, Shen W, Macdonald RL (2006) *J Neurosci* 26:2590–2597.
- Kang JQ, Macdonald RL (2004) *J Neurosci* 24:8672–8677.
- Hales TG, Tang H, Bollan KA, Johnson SJ, King DP, McDonald NA, Cheng A, Connolly CN (2005) *Mol Cell Neurosci* 29:120–127.
- Fedi M, Berkovic SF, Marini C, Mulligan R, Tochon-Danguy H, Reutens DC (2006) *Neuroimage* 32:995–1000.
- Bowser DN, Wagner DA, Czajkowski C, Cromer BA, Parker MW, Wallace RH, Harkin LA, Mulley JC, Marini C, Berkovic SF, et al. (2002) *Proc Natl Acad Sci USA* 99:15170–15175.
- Bianchi MT, Song L, Zhang H, Macdonald RL (2002) *J Neurosci* 22:5321–5327.
- Meeren HK, Pijn JP, Van Luijtelaar EL, Coenen AM, Lopes da Silva FH (2002) *J Neurosci* 22:1480–1495.
- Schwenk F, Baron U, Rajewsky K (1995) *Nucleic Acids Res* 23:5080–5081.
- Crunelli V, Leresche N (2002) *Nat Rev Neurosci* 3:371–382.
- Ferraro TN, Golden GT, Smith GG, DeMuth D, Buono RJ, Berrettini WH (2002) *Brain Res* 936:82–86.
- Ryan LJ (1984) *Brain Res Bull* 13:549–558.
- Gastaut H, Zifkin BG, Mariani E, Puig JS (1986) *Neurology* 36:1021–1028.
- Frankel WN, Beyer B, Maxwell CR, Pretel S, Letts VA, Siegel SJ (2005) *J Neurosci* 25:3452–3458.
- Steriade M (2005) *Trends Neurosci* 28:317–324.
- Pinault D (2003) *J Physiol* 552:881–905.
- Laurie DJ, Wisden W, Seeburg PH (1992) *J Neurosci* 12:4151–4172.
- Agmon A, Connors BW (1991) *Neuroscience* 41:365–379.
- Gunther U, Benson J, Benke D, Fritschy JM, Reyes G, Knoflach F, Crestani F, Aguzzi A, Arigoni M, Lang Y, et al. (1995) *Proc Natl Acad Sci USA* 92:7749–7753.
- Sisken BF, Zwick M, Hyde JF, Cottrill CM (1993) *Equine Vet J Suppl* 14:31–34.
- Lopez-Bendito G, Molnar Z (2003) *Nat Rev Neurosci* 4:276–289.
- Stein V, Hermans-Borgmeyer I, Jentsch TJ, Hubner CA (2004) *J Comp Neurol* 468:57–64.
- Essrich C, Lorez M, Benson JA, Fritschy JM, Luscher B (1998) *Nat Neurosci* 1:563–571.
- Steriade M (2001) *J Neurophysiol* 86:1–39.
- Gloor P (1979) *Epilepsia* 20:571–588.
- Badawy RA, Curatolo JM, Newton M, Berkovic SF, Macdonell RA (2006) *Neurology* 67:1018–1022.
- Hirsch JA, Martinez LM (2006) *Curr Opin Neurobiol* 16:377–384.
- Douglas RJ, Martin KA (2004) *Annu Rev Neurosci* 27:419–451.
- Blumenfeld H, McCormick DA (2000) *J Neurosci* 20:5153–5162.
- Rudolf G, Bihoreau MT, Godfrey RF, Wilder SP, Cox RD, Lathrop M, Marescaux C, Gauguier D (2004) *Epilepsia* 45:301–308.
- Gauguier D, van Luijtelaar G, Bihoreau MT, Wilder SP, Godfrey RF, Vossen J, Coenen A, Cox RD (2004) *Epilepsia* 45:908–915.
- Bessaih T, Bourgeois L, Badiu CI, Carter DA, Toth TI, Ruano D, Lambolez B, Crunelli V, Leresche N (2006) *J Neurophysiol* 96:3074–3081.
- Strauss U, Kole MH, Brauer AU, Pahnke J, Bajorat R, Rolfs A, Nitsch R, Deisz RA (2004) *Eur J Neurosci* 19:3048–3058.
- Klein JP, Khera DS, Nersesyan H, Kimchi EY, Waxman SG, Blumenfeld H (2004) *Brain Res* 1000:102–109.
- D'Arcangelo G, D'Antuono M, Tancredi V, Avoli M (2006) *Epilepsia* 47:1144–1152.
- Nagy A, Rossant J, Nagy R, Abramow-Newerly W, Roder JC (1993) *Proc Natl Acad Sci USA* 90:8424–8428.
- Brandon EP, Gerhold KA, Qi M, McKnight GS, Idzerda RL (1995) *Recent Prog Horm Res* 50:403–408.
- Moldrich RX, Giardina SF, Beart PM (2001) *Neuropharmacology* 41:19–31.
- Fedi M, Berkovic SF, Macdonell RA, Curatolo JM, Marini C, Reutens DC (July, 2007) *Cereb Cortex*, 10.1093/cercor/bhm100.